Asian Journal of Water, Environment and Pollution, Vol. 20, No. 5 (2023), pp. 79-86.
DOI 10.3233/AJW230068

Photocatalytic Degradation of Pollutants by Using Highly Surface Pd Doped on ZnO/CdS Nanocomposite: As a Model of Water Treatment

Mithal N. Mohwes, Khawla K. Jassm and Ayad F. Alkaim[1]*

Department of Chemistry, College of Science, University of Al-Muthanna, Iraq
[1]Department of Chemistry, College of Science for Women, University of Babylon, Iraq
✉ alkaimayad@gmail.com

Received June 4, 2023; revised and accepted July 21, 2023

Abstract: In the last few decades, more attention has been focussed on water treatment. In this study, an advanced catalyst Pd-doped ZnO-CdS nanocomposite was prepared using the photo deposition method. The structure and morphology of the obtained material were studied by scanning electron microscopy (SEM), transmission electron microscopy (TEM), X-ray diffraction (XRD), examining optical properties using UV-visible spectroscopy. Results of absorption show broader bands with moderated energy band gaps and improved photocatalytic properties. The photocatalytic applications show that the increase in amount of pd/ZnO-CdS nanocomposites up to 0.4 g/L increase the number of active site, but beyond 0.4 g/L there is little increase in % degradation. Therefore, the best catalyst at 0.4 g/L was used to remove BG dye. Photo catalytic activity increase was observed for Pd/ZnO-CdS nanocomposites which is about 86.6%. Photocatalytic degradation efficiency (PDE%) increases as the dye concentration decreases from 86.66% to 26.9 %. It was observed that the photo-catalytic degradation of BG dye was 86.6%–95.8% for the first four cycles. This indicates the good stability of ZnO-CdS/Pd nano-composites and could be potentially applied in the practical batch degradation.

Key words: Zinc oxide, nanocomposite, photocatalytic, hydrothermal nanoparticles.

Introduction

Nanotechnology has a vast range of implementation which makes human sustenance safer and simple. The model and development utilise are in the field of biomedicine, cosmetics, bio-imaging, bio-sensor, solar cells, health care, energy devices, optics, semi-conductor, and optical devices, space industry, agriculture, electrochemistry, catalysis, bio-technology, pharmaceuticals, textile industry, food technology, water treatment, and ceramics. For this viewpoint, different noble metal NPs such as palladium, silver, platinum, gold, selenium, and non-metallic, in-organic chromium oxide, cobalt oxide, metal oxide NPs, lanthanum oxide, cadmium oxide, and sulphur, have been widely exploited because of their eclectic electronic, magnetic, mechanical, optical, and chemical properties (Elango, 2012; Zhang et al., 2020). Zinc oxide and cadmium sulphide are very significant semiconductors, having uses in several domains such as: catalysis, electronic devices, and energy conversion. CdS, as bare and/or functionalised powder or thin film, was remarked as a versatile and efficient material (Mashkour et al., 2011; Abd et al., 2019). Composite materials were developed to tune optical properties and improve the functionality of semiconductor structures for device applications while exhibiting superior properties compared to individual components. These materials

*Corresponding Author

are advantageous because they can compensate for the shortcomings of individual components and produce synergistic effects, like efficient charge separation and improved photo stability. By adjusting the structure and interfacial interactions, different components are assembled into composite materials, achieving new properties and different functions (Alqaragully et al., 2015).

Until now, ternary nanocomposites of zinc oxide with cadmium sulphide onto Pd their morphological (nanoparticles and Nano rods) differences have not been reported in many papers for photo-catalytic antibacterial applications. Visible light-driven Pd deposited ZnO/CuO nano-structures, $ZnO/Ag_2MoO_4/Ag$ nano-composites, Fe doped ZnO/CdS nanocomposite $Ag/ZnO/Fe_3O_4$ magnetic composite (Aljeboree and Alkaim, 2019, Hashim et al., 2019) are some of the transition metal and noble metal deposited nano-composite which show ex-preemptory performance in the photo-catalytic applications. Therefore, the current research focusses on optimising the geometric parameters, design, and composition of the model to improve ZnO-CdS and Pd-doped ZnO-CdS.

Experimental Part

Methods and Materials

All chemical compounds were purchased from commercial sources and utilised as received. The reagents have top purity, were obtained from Sigma-Aldrich (cadmium acetate, $Cd(CH_3COO)_2{\cdot}2H_2O$; methanol CH_3OH; sodium sulphide Na_2S, Zinc acetate $Zn(CH_3COO)_2.2H_2O$; palladium chloride ($PdCl_2$), ***Brilliant green (BG) dye***.

Preparation of ZnO

The procedure to prepare ZnO NPs is as follows – Firstly, zinc acetate (4 g) was dissolved in 75 ml of DW, and in another beaker oxalic acid (5 g) was dissolved in 75 ml of DW. The two chemical compounds were mixed followed by a series of chemical reactions. The complete hydrolysis of zinc acetate with the oxalic acid in water resulted in the formation of a ZnO colloid. The resultant solution was transferred into the the Teflon cup, which was sealed with stainless steel followed by autoclaving. The autoclave was placed inside the oven and at a temperature of 15°C for 24 h.

Preparation of ZnO-CdS Nanocomposite

The nanocomposite (ZnO-CdS) was prepared using a hydrothermal system as shown in Figure 1. A total of

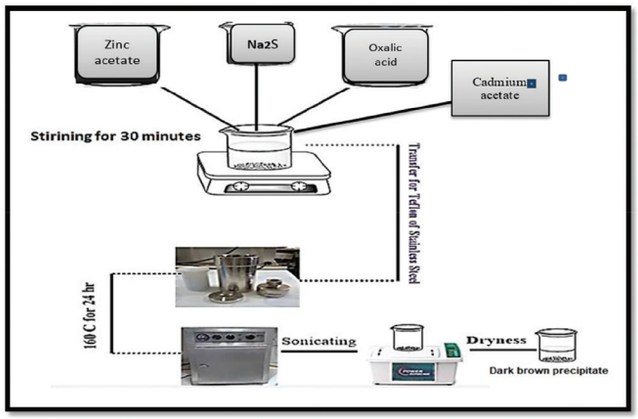

Figure 1: Suggested scheme of preparation of ZnO-CdS nanocomposite.

Note: The composite ZnO-CdS was prepared with different weights of cadmium acetate, while keeping the weights of the materials used in the preparation itself for a check. After conducting several tests, the efficiency of the surface on the dye BG was evaluated, and the results showed that the weight of a 2 gm of cadmium acetate is the most efficient for the prepared surface. The weights used in the following order: 4.5 of cadmium acetate ZnO-CdS NPs 1, 2 gm of cadmium acetate ZnO-CdS NPs 2, 1 gm of cadmium acetate ZnO-CdS NPs 3.

8 g of oxalic acid and 5 g of zinc acetate was mixed with (2 g) of cadmium acetate. This mixture was added to 1g of sodium sulphide and stirred for 30 min, then the mixture is placed in the hydrothermal system (autoclave) at 160°C for 24 hr. The obtained yellow powder precipitate was filtered, washed several time with DW more than a few times and dried for 24 hr. at 80°C to obtain powder (ZnO/CdS) nanocomposite. A documented method report in the literature was used for the preparation of ZnO–CdSNCs. The following is the reaction mechanism for the formation of ZnO–CdS NCs:

$$Zn(CH_3COO)_2{\cdot}2H_2O + NaOH \rightarrow ZnO + (CH_3COOH)_2 + H_2O \quad (1)$$

$$Cd(CH_3COO)_2{\cdot}4H_2O + Na_2S + ZnO + H_2O_2 \rightarrow ZnO\text{-}CdS + (CH_3COOH)_2 + 2H_2O + NaOH \quad (2)$$

Preparation of ZnO–CdS/Pd Nanocomposite

Pd is deposited onto ZnO-CdS nanocomposite. About 0.5 g of yellow nanopowder (ZnO-CdS) and 0.5% of $PdCl_2$ is mixed and placed in a cell quartz (v/v 1% methanol/deionised water) in a total of 100 ml deionised water. The solution stirred followed by exposing it to

nitrogen gas for 10 mins under continuous magnetic stirring, ultra-sound moving the solution for a while then irradiated it 10-12 h under ultraviolet light (major wavelength 365 nm, L.I. 23 mW/cm) with uninterrupted stirring. The powder was washed different times with DW by ultra-sound devised and dried at 65°C for 24 hr to obtain nanocomposite as shown in Figure 2.

Results and Discussion

Characterisation of Nanocomposite

X-ray diffraction (XRD) pattern of ZnO shows no other summits indicating the presence of the impurity. This is an indication that these nanoparticles of zinc oxide possess one phase. The impurity patterns are observed due to effect of calcination. Nine peaks appear at 31.7°, 34.4°, 36.2°, 47.5°, 56.5°, 62.82°, 66.4°, 67.9° and 69.10, which correspond to the (100), (002), (101), (102), (110), (103), (200), (112) and (201), respectively, reflection planes, at the same order. All the peaks diffraction can as well be suggested to the hexagonal Wurtzite structure of ZnO JCPDS card (no. 36-1451) and phase pure suggests high crystallinity due to very sharp and strong peaks.

XRD of binary nanocomposites ZnO-CdS (Figure 3) shows the main peaks of ZnO and CdS. In addition, the peaks CdS have minimal intensity in the binary nanocomposites. The cause is one fourth concentrations of CdS, set with crystalline ZnO NPs phase and too CdS has minimum crystallinity than that of ZnONPs. In Pd doped ZnO/CdS nanocomposite, the diffraction peaks only reverberate the binary structures crystalline of ZnO/CdS. However, no characteristic peak of Pd is found, may be because of least content and low intensity of Pd (Sivaranjani et al., 2021).

Technique scanning electron microscope (FE-SEM) for samples (a) ZnO NPs, (b) ZnO-Cds and (c) ZnO-CdS/Pd nanocomposite (Figure 4). It is seen that hexagonal grains are uniformly spread at the surface. Reduction in the size of the grain is observed when Pd is doped on to ZnO/CdS, while the surface grossness remains the same and is nearly symmetrical. Pd metal was found to be overlapped with ZnO-CdS nanocomposites which exhibit cubic like morphology and particle size and EDX synthesised elements of nanocomposite C, O, Zn, and Cd, which indicates the presence of Cd on nanocomposite (Bader et al., 2019, El Shafey et al., 2021; Thakur, 2018).

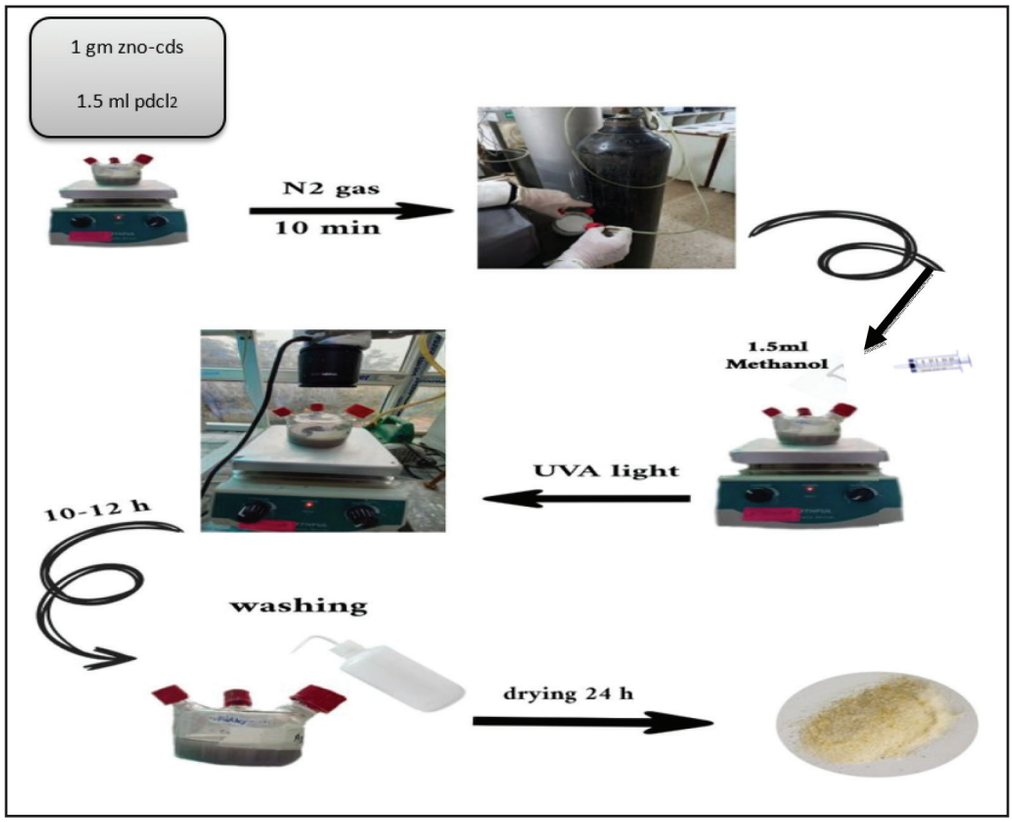

Figure 2: Suggested scheme of photochemical deposition of Pd metal on surface of ZnO–CdS.

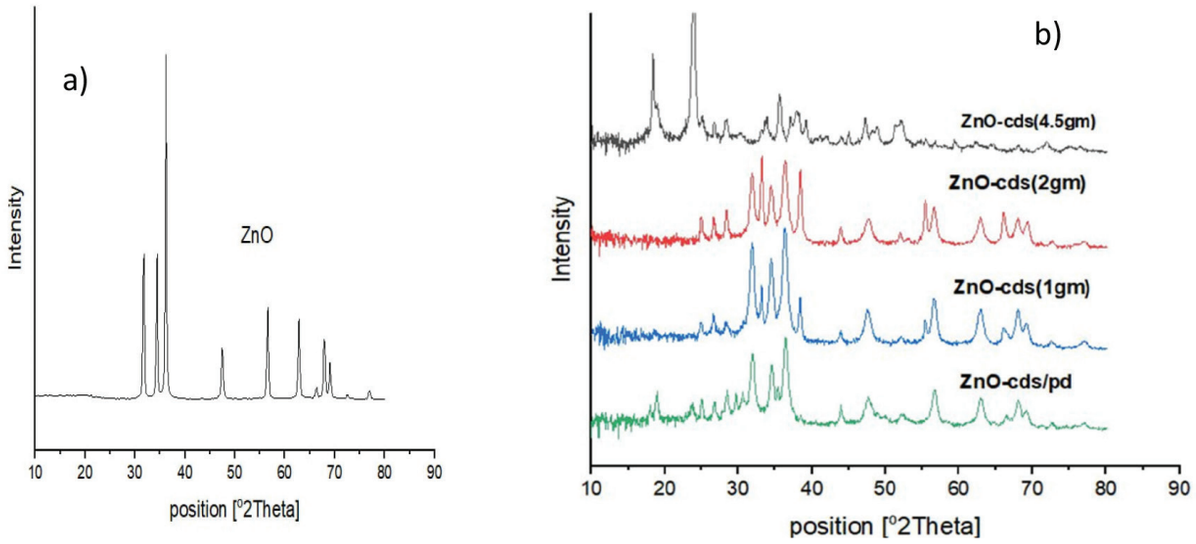

Figure 3: XRD of (a) ZnO NPs; (b) ZnO-CdS NPs (4.5 gm) , ZnO-CdS NPs (2 gm), ZnO-CdS NPs (1 gm) and ZnO–CdS\Pd.

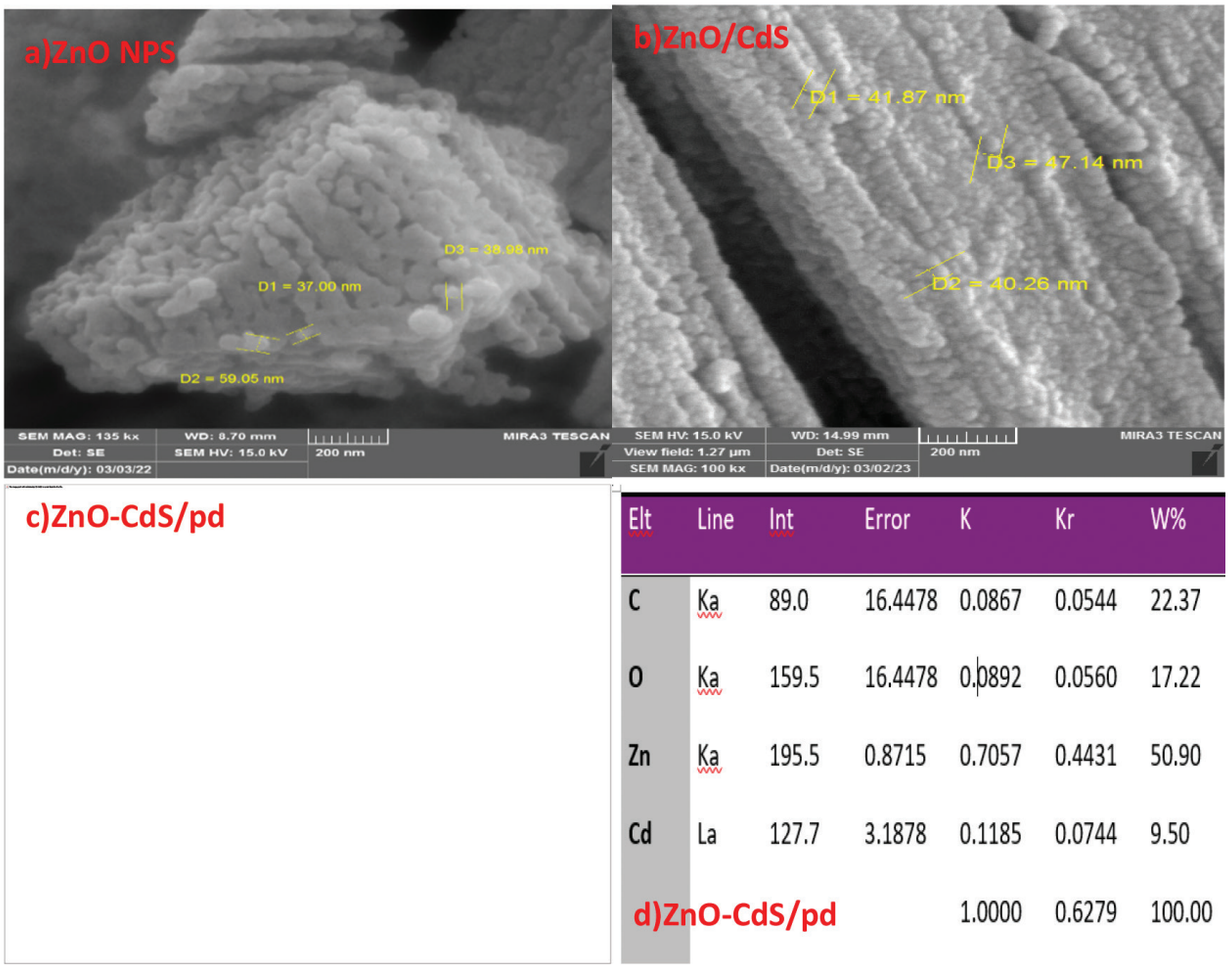

Elt	Line	Int	Error	K	Kr	W%
C	Ka	89.0	16.4478	0.0867	0.0544	22.37
O	Ka	159.5	16.4478	0.0892	0.0560	17.22
Zn	Ka	195.5	0.8715	0.7057	0.4431	50.90
Cd	La	127.7	3.1878	0.1185	0.0744	9.50
d)ZnO-CdS/pd				1.0000	0.6279	100.00

Figure 4: FE-SEM for samples (a) ZnO NPs, (b) ZnO-Cds and (c) ZnO-CdS\Pd nanocomposite and EDX (d) nanocomposite.

Transmittance electron microscopy (TEM) images were gained to limit the morphology, crystal structure and particle size of ZnO NPs and ZnO-CdS/Pd nano-composites. Figures 5a (ZnO NPs) and 5b (ZnO-CdS/Pd) show the surface particle structure of the ZnO-CdS/Pd nanocomposite which is present in a structure globular stacked. Furthermore, ZnO, CdS and Pd are stacked in close contact together. The intensive small globular dot shown in Figure 5b exemplifies the Pd ion incorporated uniformly to the ZnO-CdS surface. TEM images suggest that the Pd doping of binary ZnO-CdS was composited successfully (Aljeboree et al., 2019, Syah et al., 2021).

The band gap of semi-conductor materials strongly affect their electrical and optical properties, so it is significant to study their changes band gap for a best understanding of the pertinent particular of this type of materials. Absorption spectroscopy is a powerful tool for determining the optical properties of nanoparticles. The absorption spectra of ZnO NPs, ZnO/CdS, and ZnO-CdS/Pd nanocomposite in the UV and visible ranges at various thermal treatment temperatures are presented (Hashim et al., 2019). All spectra showed absorption edges between 370 and 390 nm, which is consistent with zinc oxide intrinsic band gap absorpat generated by electron-transitions as of valince for conduction bands (O 2 p →ZnO 3d). Figure 6 demonstrates that ZnO NPs have a larger band gap than larger spherical crystals. This can be explained by the nanoscale properties of materials (Singla et al., 2009).

Effect of Different Parameter of Photo Catalysis

Effect Concentration of Brilliant Green (BG) Dye

The influence concentration of BG dye under UV light used was in the range 25-100 mg/L in the presence of 0.4 g of ZnO-CdS/Pd nano-composite, the light intensity equal to (1.27 mW/cm^2). The results appearing in Figure 7 show that the concentration of BG dye is a limiting parameter in utmost of the removal of dyes, especially in photo degradation. As the concentration of BG dye increases, it prevents the penetration of light irradiation into the medium, so that BG dye photo degradation would be reduced remarkably, it means, the higher the concentration, the lower the dye photo degradation (Pirsaheb et al., 2016).

Figure 8 shows that the dye photocatalytic degradation efficiency (PDE%) increases as the dye concentration decreases, the PDE% increased from 95.76% to 67.98%, and this occurs either by reducing holes or (OH) because the active sites will complete the coverage with the BG or a rise in the dye concentration caused an increased adsorption of the dye on the nanocomposite, which leads to reduced (OH) radical generation, because of the low availability of the free active site on the surface (Sivaranjani et al., 2015).

Effect of Mass Nanocomposite

The effect of the photo catalyst BG dye concentration (0.1– 0.6 g/200 ml) on the photo catalytic degradation dye was studied at an initial dye. The utmost optimum

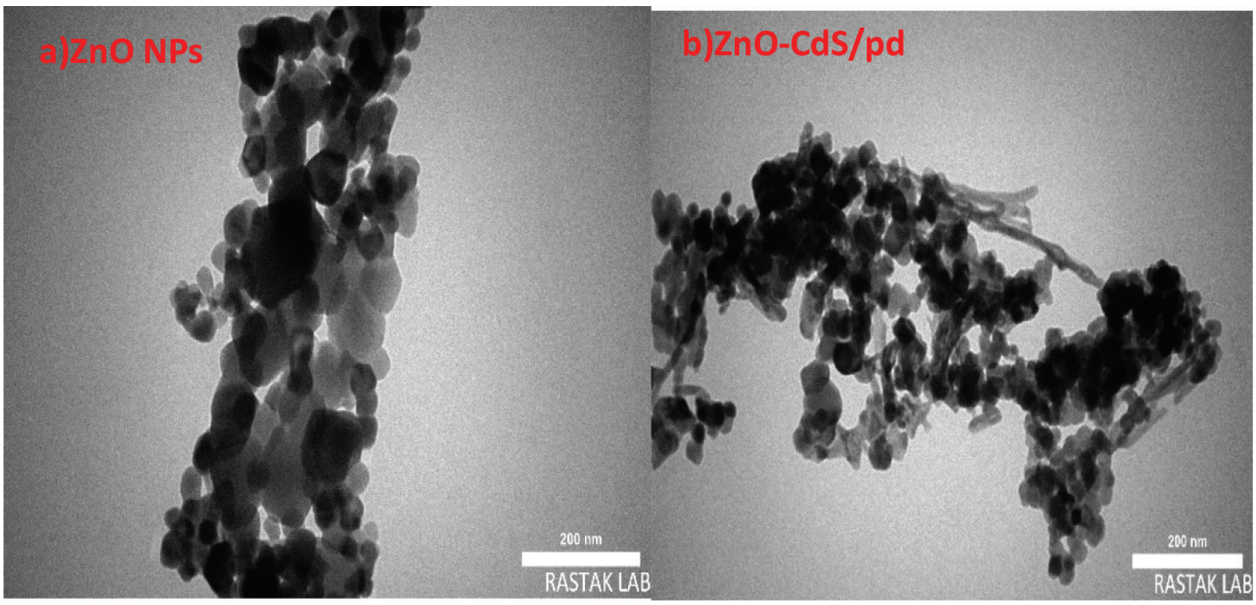

Figure 5: TEM (a) ZnO NPs, (b) ZnO-CdS/Pd nanocomposite.

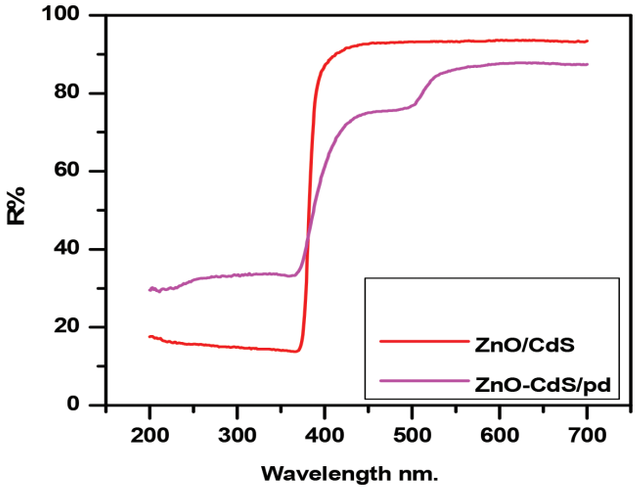

Figure 6: Effect of energy band gap of nanocomposite.

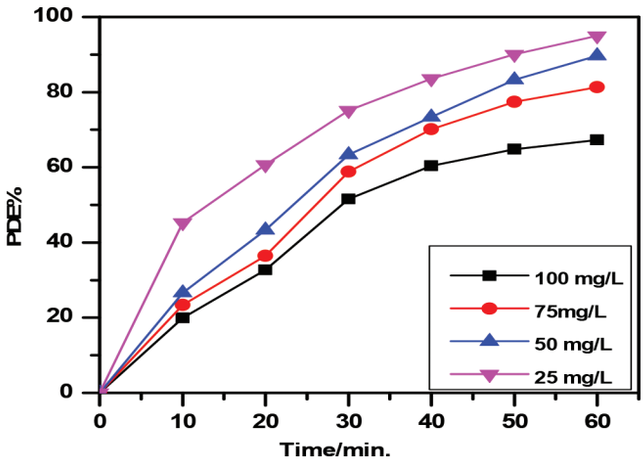

Figure 8: Effect concentration of BG dye on the PDE%.

condition BG dye concentration of light intensity are 2.7 mW/cm^2, 50 mg/L, and solution pH 6.8, as shown in Figure 9.

When the mass nanocomposite was increased, the rate degradation increased too because of the increase in number of active sites. In the region among 0.1-0.6 g, appear an approximately plateau curve which indicates the numbers of active sites have an equilibrium among the numbers of photon induced that absorbed via the catalyst and a particle of dye adsorbed represents the percent degradation of dye against the quantities of nanocomposite (Karam et al., 2015). This shows that the percent degradation of modified catalysts rise with increase in amount of catalyst from 0.1 to 0.6 g·L^{-1} and above this limit there is not much change as shown in Figure 10.

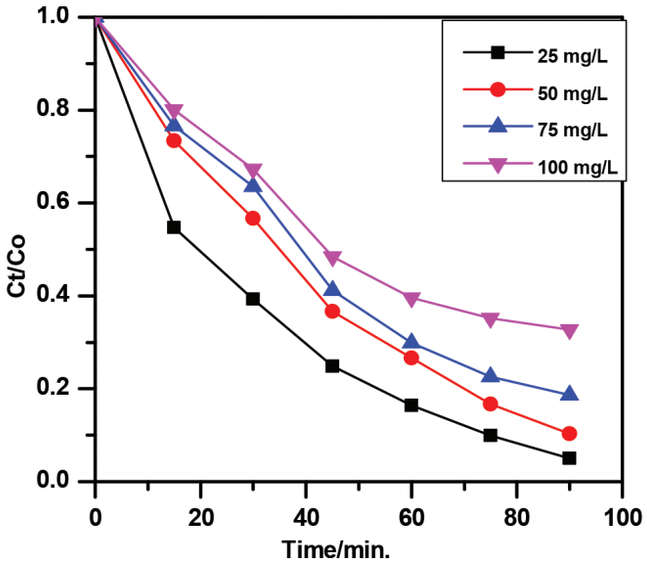

Figure 7: Effect of photocatalytic degradation by nanocomposite at different concentration of BG dye.

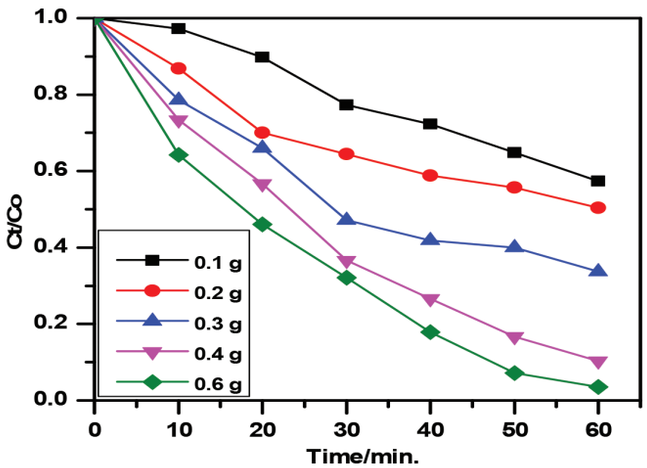

Figure 9: Photo catalytic degradation of BG dye at different weight of nanocomposite.

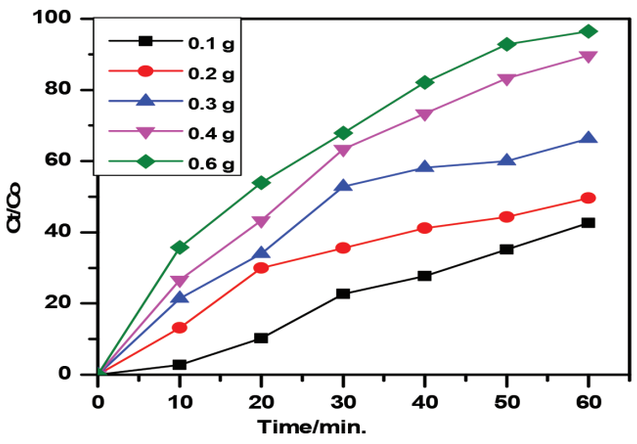

Figure 10: PDE% MB at several weight of nanocomposite.

Re-usability and Stability of Nano-composites

The estimate of photo stability and immovability of the photo catalyst under a repetitive photo-catalytic cycle is the main for practical implementation. Re-cyclability of Pd doped ZnO-CdS nano-composites was examined for five cycle as appears in Figure 11. This nano-composite catalyst is washed several times in distilled water after that dried in oven at 60°C. It can be seen that the photo-catalytic activity of nano-composites was decreased a little to 2.2% after five cycles sequential. It was observed that the photo-catalytic activity of BG were 86.6%, 85.9%, 84.9%, 83.6%, 82.2%, 80% and 77.1%. for first, to six cycles at the same order. This marked the best stability of nano-composites and could be potentially used in photo degradation.

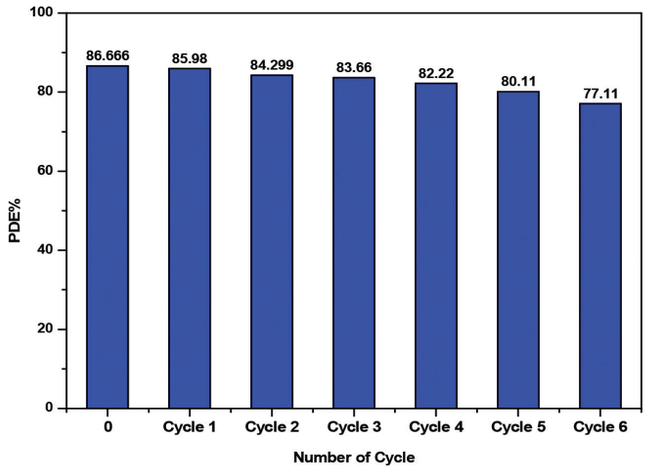

Figure 11: Effect of reusability and stability nanocomposites.

Conclusion

1. ZnO/CdS was prepared using the modified hydrothermal process, Pd doped ZnO/CdS, were prepared by a photo deposition method.
2. The concentration of BG dye 50 mg/L gives the best photocatalytic degradation capacity 86.66%.
3. Photocatalytic degradation efficiency (PDE%) increases as the dye concentration decreases from 86.66 % to 26.9%.
4. Photo catalytic degradation increases with increasing mass of catalyst nanocomposite, but decreases with increased concentration of BG dye.
4. The nanocomposite surface shows a high stability and the powder can be used several times.

References

Abd, L.H., Abbas, R., Aljeboree, A.M., Abdulrazzak, A.M., Hussein, F.H. and A.F. Alkaim (2019). Role of semiconductors (zinc oxide as a model) for removal of pharmaceutical tetracycline (TCs) from aqueous solutions in the presence of selective light. *International Journal of Recent Technology and Engineering*, **8(23):** 1461-1463.

Abdulrazzak, F.H., Jawad, M.A., Alkadir, O.K.A. and A.F. Alkaim (2021). Antimicrobial activity of Ag:ZnO/MWCNT against *Cinetobacter baumannii*. *Journal of Nanostructures*, **11(2):** 317-322.

Algubili, A.M., Alrobayi, E.M. and A.F. Alkaim (2015). Photocatalytic degradation of remazol brilliant blue dye by ZnO/UV process. *International Journal of Chemical Sciences*, **13(2):** 911-921.

El Shafey, A.M., Abdel-Latif, M.K. and H.M. Abd El-Salam (2021). The facile synthesis of poly(acrylate/acrylamide) titanium dioxide nanocomposite for groundwater ammonia removal. *Desalination and Water Treatment*, **212:** 61-70.

Aljeboree, A.M. and A.F. Alkaim (2019). Role of plant wastes as an ecofriendly for pollutants (crystal violet dye) removal from aqueous solutions. *Plant Archives*, **19:** 902-905.

Aljeboree, A.M., Alshirifi, A.N. and A.F. Alkaim (2019). Activated carbon (as a waste plant sources)-clay micro/nanocomposite as effective adsorbent: Process optimization for ultrasound-assisted adsorption removal of amoxicillin drug. *Plant Archives*, **19:** 915-919.

Alqaragully, M.B., Al-Gubury, H.Y., Aljeboree, A.M., Karam, F.F. and A.F. Alkaim (2015). Monoethanolamine: Production plant. *Research Journal of Pharmaceutical, Biological and Chemical Sciences*, **6(5):** 1287-1296.

Bader, A.T., Zaied, A.M. Aljeboree, A.M. and A.F. Alkaim (2019). Removal of methyl violet (MV) from aqueous solutions by adsorption using activated carbon from pine husks (plant waste sources). *Plant Archives*, **19:** 898-901.

Elango, M., Nataraj, D., Prem Nazeer, K. and M. Thamilselvan (2012). Synthesis and characterization of nickel doped cadmium sulfide (CdS:Ni^{2+}) nanoparticles. *Materials Research Bulletin*, **47(6):** 1533-1538.

Hashim, F.S., Alkaim, A.F., Mahdi, S.M. and A.H. Omran Alkhayatt (2019). Photocatalytic degradation of GRL dye from aqueous solutions in the presence of ZnO/Fe_2O_3 nanocomposites.*Composites Communications*, **16:** 111-116.

Hashim, F.S., Alkaim, A.F., Salim, S.J. and A.H.O. Alkhayatt (2019). Effect of (Ag, Pd) doping on structural, and optical properties of ZnO nanoparticales: As a model of photocatalytic activity for water pollution treatment. *Chemical Physics Letters*, **737:** 136828.

Kaliyappan Sivaranjani, K., Sivakumar, S. and J. Dharmaraja (2022). Enhancement photocatalytic activity of Mn doped CdS/ZnO nanocomposites for the degradation of methylene blue under solar light irradiation. *Advances in Materials Science*, **22(2):** 28-48.

Karam, F.F., Kadhim, M.I. and A.F. Alkaim (2015). Optimal conditions for synthesis of 1, 4-naphthaquinone by photocatalytic oxidation of naphthalene in closed system reactor. *International Journal of Chemical Sciences*, **13(2):** 650-660.

Mashkour, M.S., Al-Kaim, A.F., Ahmed, L.M. and F.H. Hussein (2011). Zinc oxide assisted photocatalytic decolorization of reactive red 2 dye. *International Journal of Chemical Sciences*, **9(3):** 969-979.

Pirsaheb, M., Shahmoradi, B., Khosravi, T., Karimi, K. and Y. Zandsalimi (2016). Solar degradation of malachite green using nickel-doped TiO_2 nanocatalysts. *Desalination and Water Treatment*, **57(21):** 9881-9888.

Singla, M.L., Shafeeq, M. and M. Kumar (2009). Optical characterization of ZnO nanoparticles capped with various surfactants. *Journal of Luminescence*, **129(5):** 434-438.

Syah, R., Altajer, A.H., Abdul-Rasheed, O.F., Tanjung, F.A., Aljeboree, A.M., Alrazzak, N.A. and A.F. Alkaim (2021). $CuMoO_4$/ ZnO nanocomposites: Novel synthesis, characterization, and photocatalytic performance. *Journal of Nanostructures*, **11(1):** 73-80.

Thakur, S. (2018). Synthesis, characterization and adsorption studies of an acrylic acid-grafted sodium alginate-based TiO_2 hydrogel nanocomposite. *Adsorption Science & Technology*, **36(1-2):** 458-477.

Zhang, B.,. Jabarullah, N.H., Alkaim, A.F., Danshina, S., Krasnopevtseva, I.V., Zheng, Y. and N. Geetha (2020). Thermomechanical fatigue lifetime evaluation of solder joints in power semiconductors using a novel energy based modeling. *Soldering and Surface Mount Technology*, **33(3):** 187-194.